

The Comparison between Full-Stack Data and Pure P-Wave Data on Deeply Buried Ordovician Paleokarst Reservoir Prediction

Yuanyin Zhang^{1,2,3,4}, Zhijun Jin^{1,2,3}, Zandong Sun^{4,5} & Chunyan Fan⁴

¹ Petroleum Exploration and Production Research Institute, SinoPEC, Beijing, China

² Sinopec Key Laboratory of Shale Oil/Gas Exploration and Production Technology, Beijing, China

³ National energy R & D center of shale oil, Beijing, China

⁴ China University of Petroleum Beijing, China

⁵ PetroChina Tarim Oilfield Co. CNPC

Correspondence: Yuanyin Zhang, Petroleum Exploration and Production Research Institute, SinoPEC, No. 31 Xueyuan Road, Haidian District, Beijing, China. Tel: 86-1510-1173-579. E-mail: yuanyinshou@163.com

Received: November 21, 2015

Accepted: December 9, 2015

Online Published: January 10, 2016

doi:10.5539/esr.v5n1p57

URL: <http://dx.doi.org/10.5539/esr.v5n1p57>

Abstract

The present burial depth of the paleokarst reservoirs in the Tarim Basin is greater than 5000m, which premises rigorous demands for the data quality for accurate predictions. Although routinely used for reservoir prediction, the conventional full-stack data are often contaminated by the AVO (amplitude versus offset) effects no matter how much signal to noise ratio degree can be enhanced via stacking. This contamination usually changes with different geological deposits, and could reach an inappropriate and unacceptable level for the deeply buried carbonate reservoir in the Tarim Basin. In this paper, the pure P-wave data theoretically inverted through AVO effects removal are employed to improve reservoir prediction, which are illustrated by the comparisons with that of the conventional full-stack data for the classical four AVO models and the field data in the ZG8 area, Tazhong Uplift, central Tarim Basin. The dominant frequency has been improved for 8 Hz from 15 to 23 Hz in the target Yingshan formation, Ordovician through AVO effects removal, and the reflection events of the pure P-wave data are obviously more continuous comparing with that of the full-stack data. The fake potential reservoir caused by AVO effects in the northeast area has been removed, while the integral delineation of paleokarst reservoirs have been significantly improved with a higher fitness with the oil-testing results, which are more beneficial for later on exploration. The pure P-wave data inversion is in essence an important complement to current processing strategy.

Keywords: paleokarst, reservoir characterization, AVO effects, P-wave data, Tarim Basin

1. Introduction

Paleokarst reservoirs are uncommon worldwide but can contain significant hydrocarbons reserves (Tinker et al., 1995; Kerans, 1988; Dembicki & Machel, 1996; Chen et al., 2005; Janson et al., 2010). In the Tarim Basin in Western China, the Ordovician karst play is actively producing hydrocarbons and reserves approximately 72.84% of the whole hydrocarbon resources (Ping et al., 2007). With two strong tectonic movements during the Early and Late Paleozoic, the Ordovician carbonate rocks experienced strong weathering and erosion and formed a karst reservoir, which is overburdened by Carboniferous and Triassic clastic rock. The present burial depth of the karst reservoirs in the Tarim Basin is greater than 5000m (Yang et al., 2010). Because of this deep burial and compaction, large voids that are associated with paleokarst chambers would be unusual in the Ordovician sequence because these features generally collapse and disappear beyond 3000m of burial (Loucks, 1999). In addition, core analyses indicate that the matrix porosity in conventional cores is extremely low (<2%), and the storage spaces are dissolution pores and fractures (Sun et al., 2012). Consequently, widespread strong reflection amplitudes that are related to high reflection coefficients at brine-hydrocarbon fluid contacts, which are typical in shallow porous unconsolidated reservoirs, are not expected (Zeng et al., 2011). On the contrary, anomalously strong seismic amplitudes that frequently occur in the Middle and Lower Ordovician succession beneath the top Ordovician unconformity are characteristic of the Tarim Basin. These anomalous amplitudes are associated with high-velocity limestone matrix and low-velocity reservoirs and are often regarded as the best indicator of good

reservoirs. Zhang et al. (2011a) suggested that a dissolution reservoir with a low velocity compared to the tight carbonate matrix can be recognized at the seismic scale if its dissolution thickness is larger than 35 m because the reservoir could then be imaged clearly in the post-stack seismic section. However, the seismic data quality is the fundamental factor which dominates the reservoir prediction.

Although routinely used for reservoir prediction, the conventional full-stack data are usually contaminated by AVO effects no matter how much signal to noise ratio (SNR) degree can be enhanced via stacking (Zhang et al., 2013; Han et al., 2013). This contamination often changes with different geological deposits, and could reach an inappropriate level for the deeply buried carbonate reservoir in the Tarim Basin. Nevertheless, there are few discussions on the characterization difference for the deeply buried Ordovician Paleokarst reservoir in that area using the pure P-wave data and the conventional full-stack data. The predicted reservoir distributions from the full-stack data do have made great contributions over the past two decades, but are gradually reported to be not qualified for the current elaborate exploration. In this paper, the pure P-wave data theoretically inverted through AVO effects removal are employed to improve the reservoir prediction, which are illustrated by the comparisons with that of the conventional full-stack data for the classical four AVO models and the field data in the ZG8 area, Tazhong Uplift, central Tarim Basin.

2. Background Geology

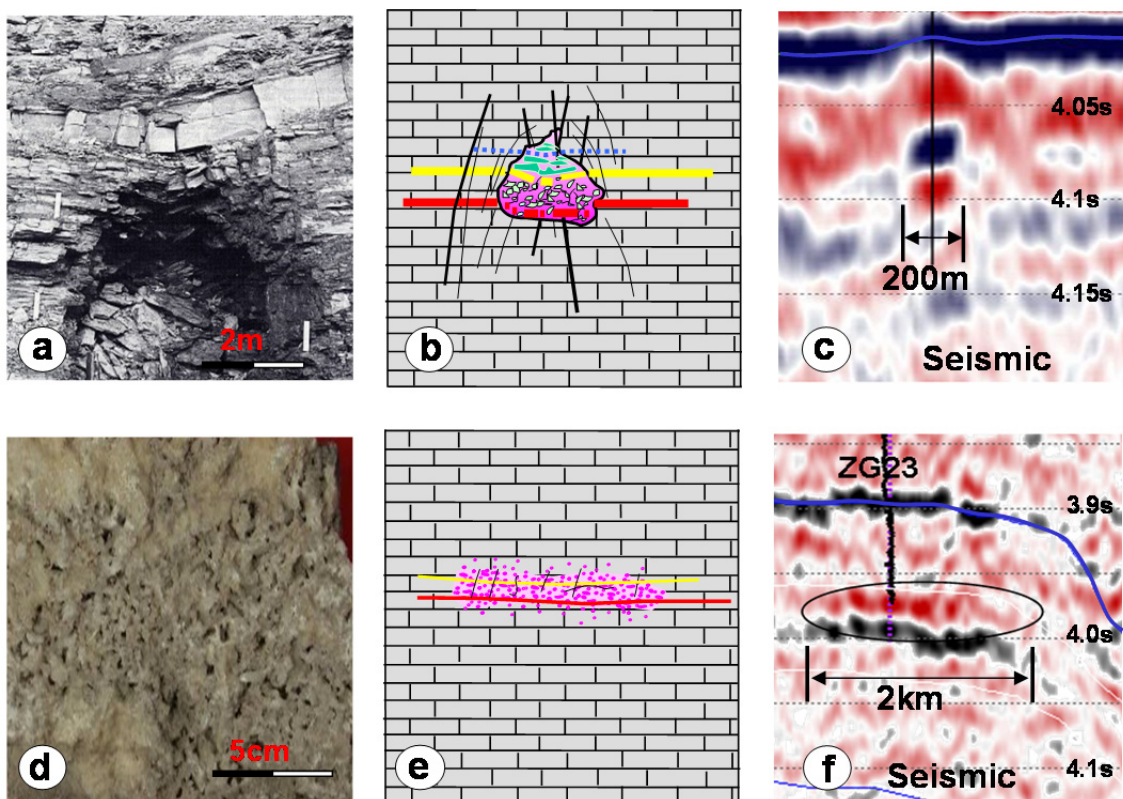


Figure 1. The core picture, structure model and corresponding post-stack seismic reflection for typical “bead-like reflection” (BR) (a, b and c) and “flake-like reflection” (FR) (d, e and f) reservoir in the Tarim Basin. The red and yellow colors in the schematic structure model map (b and e) indicate oil and gas respectively, while vertical dark lines stand for classic strike-slip faults in this field. The blue line in seismic section (c and f) is the top of carbonate strata. The BR is mainly formed by resolvable dissolution caves, while the counterpart FR is principally composed by tiny dissolution vugs

Karstified Ordovician limestone in the Tarim Basin has been shown to be a highly productive oil and gas reservoir (Sun et al., 2011a; Yang et al., 2012). The limestone is substantially dense and exhibits a high seismic velocity because of its deep burial (>5000 m). Anomalously strong seismic amplitudes in the Middle and Lower Ordovician succession beneath the top Ordovician unconformity associated with high-velocity limestone matrix

and low-velocity reservoirs are often regarded as the best indicator of good reservoirs. In particular, the anomalously strong seismic amplitudes in the Tarim Basin can be roughly classified into two types, including bead-like reflections (BRs, often called lamb kebabs) (Figure 1c) and flake-like reflections (FRs) (Figure 1f) (Zhang et al., 2011b). The BRs that are characterized as substantial strong amplitudes with relatively small lateral ranges are primarily formed by seismically resolvable dissolution caves, which have made great contributions to hydrocarbon producing over the past two decades (Zhang et al., 2011a; Zeng et al., 2011; Yang et al., 2012). On the other hand, the FRs that are composed by strong amplitudes with wider lateral ranges are mainly formed by extensively distributed tiny dissolution vugs, which are also capable of developing good reservoirs.

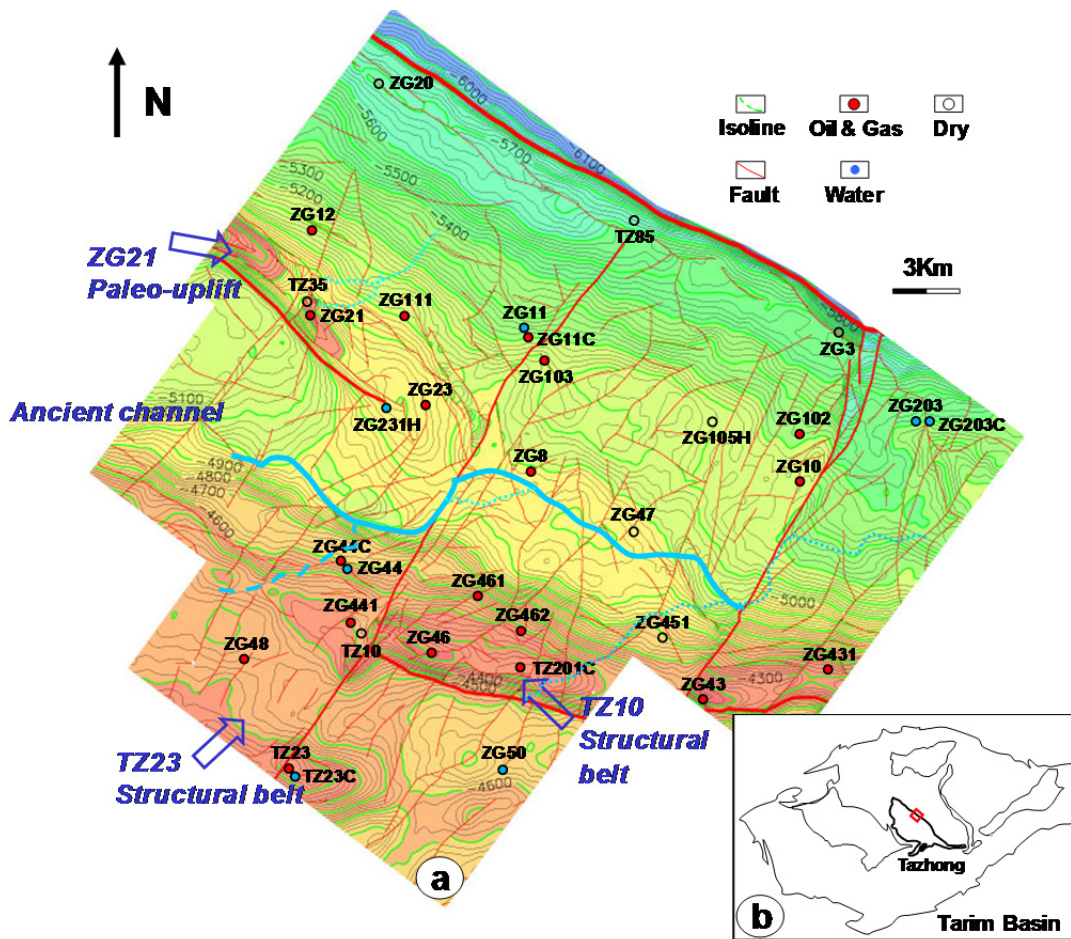


Figure 2. The geological setting and exploration status of ZG8 area (a), as well as its location in the Tarim Basin (b). The colorful background and contours are the top of Yingshan formation (To3l), Ordovician, suggesting that the current carbonate structure gradually plunges from the southwest (SW) into the northeast (NE). The interpreted ancient channel system is depicted by baby blue color, while the width of red lines represents the intensity and scale of faults. Hydrocarbon producing wells are mainly distributed in the high stratigraphic trappings (including TZ23, TZ10 structural belts and ZG21 paleo-uplift) along the two big strike-slip faults from SW to NE

The study ZG8 area in the Tarim Basin locates at the north central Tazhong Uplift, which is a large anticline that is bounded by reverse fault in the northeast (TZ I fault zone) and by the anticline dip to the south and southwest (Figure 2b), with a slope of 1 to 2 degree (Zeng et al., 2011). Paleogeomorphology analysis in the Ordovician suggests that the ancient landform is formed by three belts including karst highland, karst inclining, and karst depression from the southwest (SW) to the northeast (NE) (Yang et al., 2012). Besides, the Ordovician paleokarst reservoir succession in ZG8 area is characterized as a product of complex karstification that is related to a paleokarst drainage system and subsequent tectonic disruption during burial (Zeng et al., 2011). The ancient

water system meandered from the west to the east (baby blue color in Figure 2a) and the strike-slip faults from the SW to the NE (red color in Figure 2a) are found to be highly related to good paleokarst reservoirs. (Jia et al., 1998; Yang et al., 2012). Aiming at the bead-like-reflection reservoirs, the current hydrocarbon producing wells are primarily deployed in the high stratigraphic trappings along the two big strike-slip faults from the SW to the NE and the three fertile uplifts consisted of TZ23, TZ10 structural belts and ZG21 paleouplift (Figure 2a) (Zhang et al., 2011b; Yang et al., 2012). On the other hand, the paleokarst depression in the northeast (well ZG20, TZ85 and ZG3) with a lager burial is not appropriate to develop good reservoir (Zhang et al., 2011b; Yang et al., 2012). However, reservoir distribution in the rest area (i.e., paleokarst inclining) predicted by the conventional full-stack seismic data is not accurate, which results in the failure of two latest wells in the north-central (well ZG47 and ZG105H).

3. Method

3.1 Full-Stack Data and Pure P-Wave Data

For the improvement of seismic data SNR in the current multiple-fold acquisition system, it is a common practice to stack all the traces of a common-reflection-point (CRP) as the so-called zero-incident data for interpretation enhancement (Han et al., 2013). For n traces in a CRP (after pre-stack migration), the conventional full-stack data are often computed by:

$$Stack = \sum_{i=1}^n S_{pp}(\theta_i) / n \quad (1)$$

Where, $S_{pp}(\theta)$ is the seismic reflection with ray-path of incident angle, and θ is the average of incidence and transmission angles.

However, this process has made a reluctant compromise to the sacrifice of data resolution and accuracy due to the contamination of AVO effects no matter how much SNR degree could be enhanced (Zhang et al., 2013). To overcome this shortcoming, the P-wave data is theoretically inverted in this paper through AVO effects removal via pre-stack AVO inversion. The most useful form of the pre-stack inversion formula (Gidlow et al., 1992) can be reorganized from Aki & Richards equation and illustrated as follow:

$$R_{pp}(\theta) = (1 + \tan^2 \theta) R_p - 8 \frac{V_s^2}{V_p^2} R_s \sin^2 \theta - \left(\frac{1}{2} \tan^2 \theta - 2 \frac{V_s^2}{V_p^2} \sin^2 \theta \right) \frac{\Delta \rho}{\rho} \quad (2)$$

Where, R_p and R_s are theoretical zero-offset P-wave reflectivity and S-wave reflectivity respectively,

$$R_p = \frac{1}{2} \left(\frac{\Delta \rho}{\rho} + \frac{\Delta V_p}{V_p} \right), \quad R_s = \frac{1}{2} \left(\frac{\Delta \rho}{\rho} + \frac{\Delta V_s}{V_s} \right) \quad (3)$$

And V_p , V_s and ρ are the average P-wave velocity, S-wave velocity and density of the reflection boundary. θ is the average of incidence and transmission angles. $R_{pp}(\theta)$ is the elastic reflectivity with ray-path of incident angle, $\Delta \rho / \rho$ is the density gradient. V_s / V_p is the S-to-P-wave velocity ratio.

The P-wave result is comparatively stable since the coefficient of R_p is usually bigger than that of R_s or $\Delta \rho / \rho$, and has nothing to do with V_p / V_s in the solving of upper non-linear equations (Zhang et al., 2013). If the wavelets are not removed in the inversion process, the computed R_p could be then seen as inverted P-wave data, which also used to be named as intercept.

3.2 Numerical Comparison

To demonstrate the difference between the upper two, the classical four AVO anomalies associated with gas sands normally encountered in exploration (the left panel in Figure 3) (Rutherford & Williams, 1989; Castagna et al., 1998) are employed to forward the synthetic AVO gathers by using a Ricker wavelet. The subsequent full-stacked and R_p data are computed for further comparison in Figure 3 by equation (1) and (2), respectively. In particular, the response at zero-offset (or zero incidence angle) actually indicates the pure P-wave data with the same exciting and receiving coordinates. As shown in the right panel of Figure 3, the full stack data averaged from different offsets (or incidence angles) do deviate from the zero-offset data for all the four models. And the deviations vary versus both different AVO types and incidence angle range. The corresponding errors could reach an unacceptable level to inevitably distort the original geology for Class II and Class III AVO anomalies (b and c), although the synthetic gathers are absolutely-preserved without any attenuation or noise problems. By

contrast, the inverted pure P-wave data with AVO effects removal via pre-stack inversion are almost same as the zero-offset data, and are certainly more helpful for reservoir description.

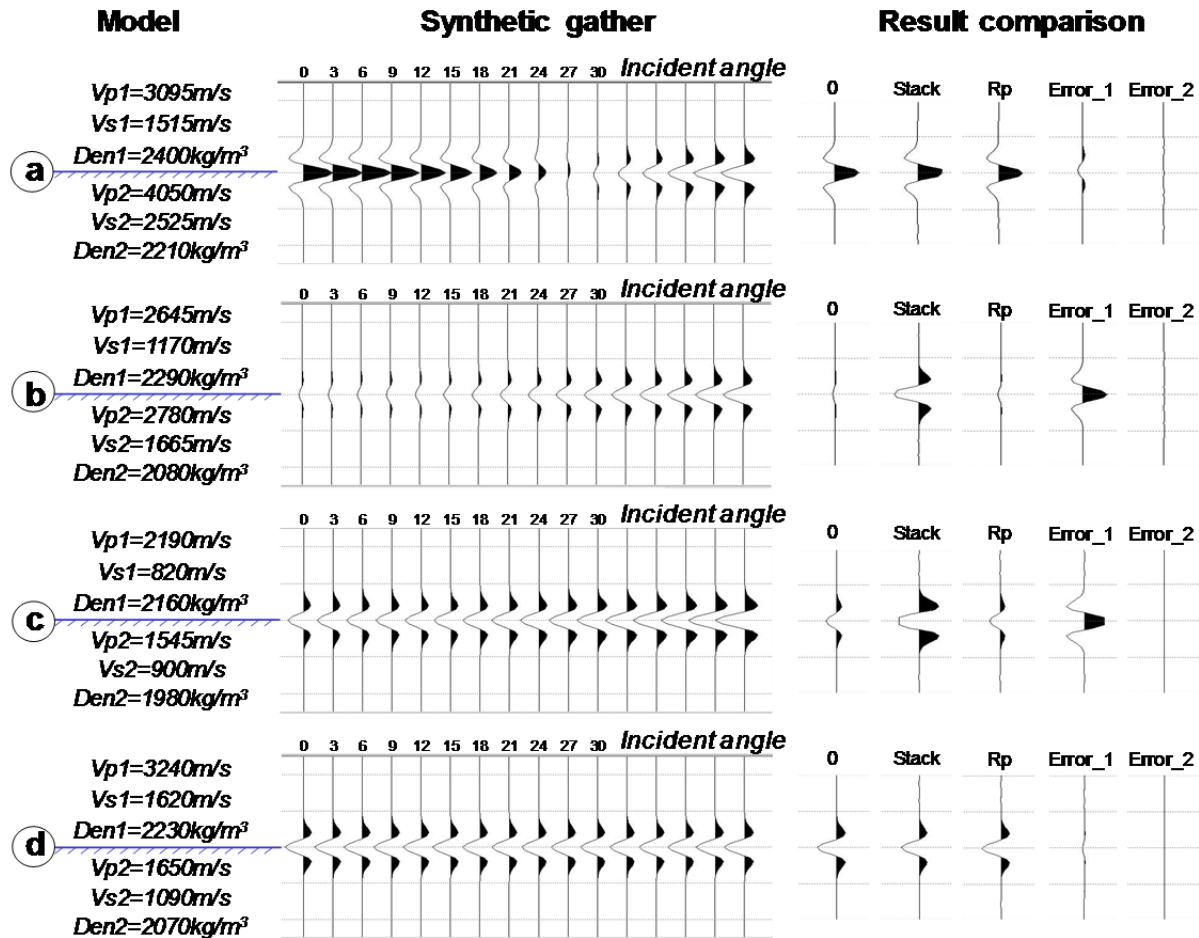


Figure 3. Comparison of zero-offset P-wave data (0), inverted P-wave data (Rp) and conventional full stack data (Stack) for four types of AVO anomalies (a-d). Error_1 and Error_2 are the differences between 0 and Stack, 0 and Rp data, respectively. Note the deviations between stack and pure P-wave data are different for different AVO anomalies

3. Comparison on Field Data

Based on the three qualified partial angle stacks (3-13, 13-23 and 23-33 degree) via pre-stack AVO inversion in ZG8 area, Tazhong Uplift, the pure P-wave data are achieved to compare with conventional full stack data on the reservoir characterization. The pre-stack AVO inversion results demand both high quality input data and high-efficiency inversion algorithms. The successful data processing in this area often focuses on preserving the true amplitudes in the whole processing workflow, e.g., amplitude compensation, noise attenuation, resolution enhancement and pre-stack migration. Significantly, the basic criterion for preserving amplitude is that the AVO characteristics between synthetic and obtained gathers should be similar (Sun et al., 2011b; Zhang et al., 2011a; Zhang et al., 2011b; Feng et al., 2012; Wang et al., 2012). Meanwhile, the pre-stack seismic inversion should be carefully applied by seriously controlling the quality of four major approaches, including angle partial stack data preparation, wavelet estimation, low-frequency model building and inversion parameter control (Zhang et al., 2011a; Zhang et al., 2011b). Theoretically, the pure P-wave data are prone to be more precisely achieved than other elastic parameters, i.e., S-wave data and density data (Zhang et al., 2013).

Figure 4 illustrates a comparison between the full-stack data and the inverted pure P-wave data across a typical line in the northeast ZG8 area. The dominant frequency has been improved for 8 Hz from 15 (Figure 4b) to 23

(Figure 4d) Hz in the target Yingshan formation, Ordovician through AVO effects removal, and the reflection events of the pure P-wave data are obviously more continuous comparing with that of the full-stack data. In fact, the reserve quality in that area used to be overestimated from the full-stack data, which took the main responsibility for the failure of well ZG105H. The area marked by a green ellipse in Figure 4a was once regarded to develop a set of potential “flake-like-reflection” reservoir, yet substantially it is shown as the AVO effects contamination caused by the upper strong reflection. This contamination has been successfully removed in the inverted P-wave data (the green ellipse marked in Figure 4c), which are definitely more beneficial for reservoir characterization.

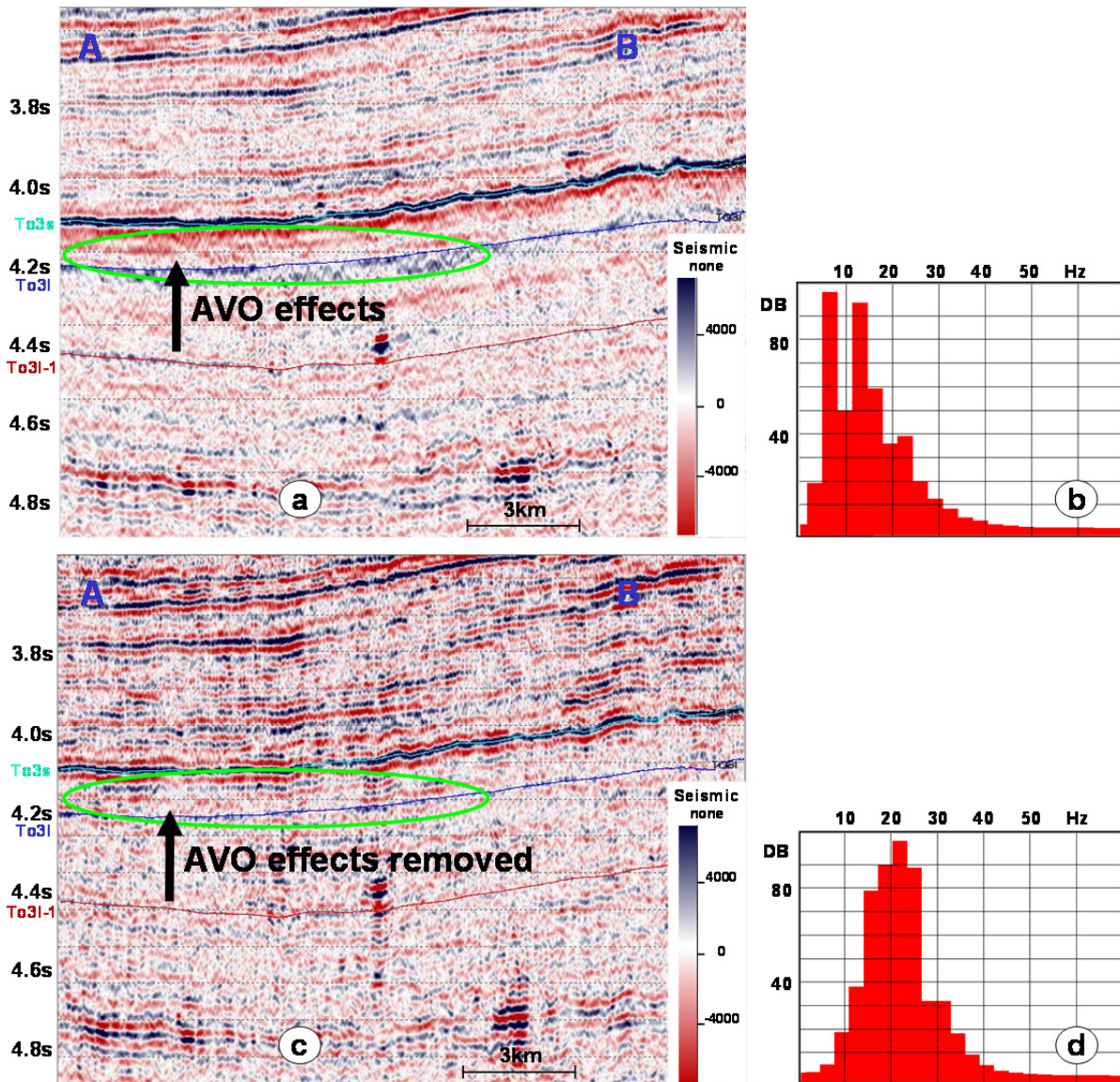


Figure 4. The comparison between the typical full-stack section (a) and the inverted P-wave section (c) in the ZG8 area across the blue line AB in Figure 6. The inverted P-wave section has more clear and continuous events, and has 8Hz dominant frequency enhanced comparing with the full stack data (b and d) in the target Yingshan formation, Ordovician. The blue and red lines are the top (To31) and base (To31-1) of the first part of Yingshan formation, respectively. The babe blue color indicates the top (To3s) of carbonate strata

As the inverted impedance has not only eliminated the wavelet influence but also added the drilling information in the initial earth model, it is widely suggested to be better correlated with the reservoir quality than seismic amplitude (Zhang et al. 2011a, Ping et al. 2007). We conduct the impedance inversion for both the full-stack and

the inverted P-wave data in ZG8 area, and the good carbonate reservoir often renders a lower impedance value comparing with that of the compacted carbonate matrix. The wavelets for two set of data are respectively extracted within the upper carbonate strata where we have reliable logging data (from the top of carbonate strata (To3s) to the top of Yingshan formation (To3l)), thus the estimated wavelets are dominated by the strong reflection at To3s horizon. The AVO anomaly at the top of carbonate strata (To3s) is not obvious, so the corresponding reflected events for the full-stack and pure P-wave data are close to each other, which decreases the frequency difference of the two extracted wavelets. As shown in Figure 5, the wavelets for two sets of data are stable and similar to the Ricker's wavelet, indicating the rationality of former amplitude-preserved processing. In particular, the frequency width from the inverted pure P-wave data is slightly wider than that from the conventional full-stack data (the black arrowhead in Figure 5b), while the phase distribution within the effective frequency band (8-40Hz) is more stable (Figure 5c) after the AVO effects removal.

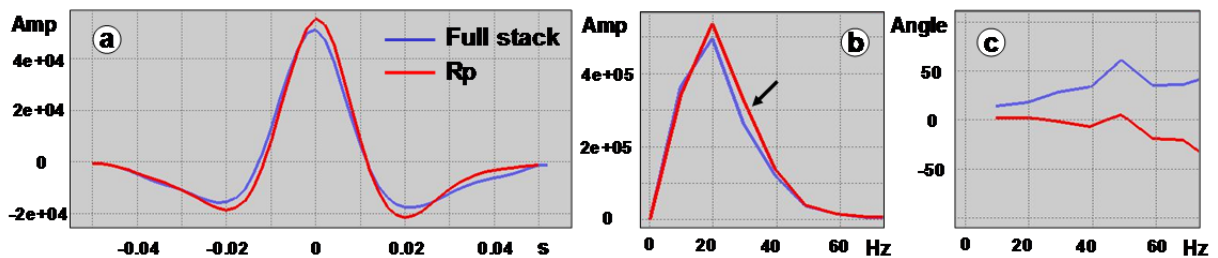


Figure 5. The estimated Wavelet shape (a), amplitude spectrum (b) and phase spectrum (c) for full-stack data (blue) and inverted P-wave data (red)

The inverted impedance of the pure P-wave data (Figure 6b) is more correlative to the drilling results, which suggests the significant reservoir characterization improvement. Sun et al. (2011a) pointed out that the compressibility differences of different porous fluids in this area are relatively unclear and very small comparing with the huge compressibility of limestone matrix, therefore the water-bearing and oil- & gas-bearing reserving spaces are similar on P-wave responses and cannot be easily distinguished. However, the P-impedance is competent for differentiating reservoir and non-reservoir. As shown in Figure 6, according to the new result, good paleokarst reservoirs are still developed in the high stratigraphic trappings (including TZ23, TZ10 structural belts and ZG21 paleo-uplift), ancient channel or along the strike-slip faults from SW to NE, whereas the so-called potential “flake-like reflection” reservoir in northeast central area in essence is the contamination of AVO effects (no commercial hydrocarbons found in the well ZG47 and ZG105H). Meanwhile, TZ10 structural belt especially in the southern part is no longer as affluence as that predicted by the full-stack data, while some local reservoirs heterogeneously distributed in TZ23 structural belt are arisen by the resolution enhancement. The oil- & gas-producing well ZG461, the dry well ZG47 and ZG105H are all incorrectly delineated by the conventional full-stack result (Figure 6a), but they are precisely identified by the inverted pure P-wave result properly. Although this reservoir prediction enhancement seems not extensively remarkable in an entire statistical fitting rate for 34 oil-testing results, it makes a significant contribution for the elaborate reservoir appraisalment in the central northeast part. This result is also more beneficial for improving reservoir understanding and making appropriate exploration strategies, which is eagerly required for production equipment of 4 million ton and well deployment in that area.

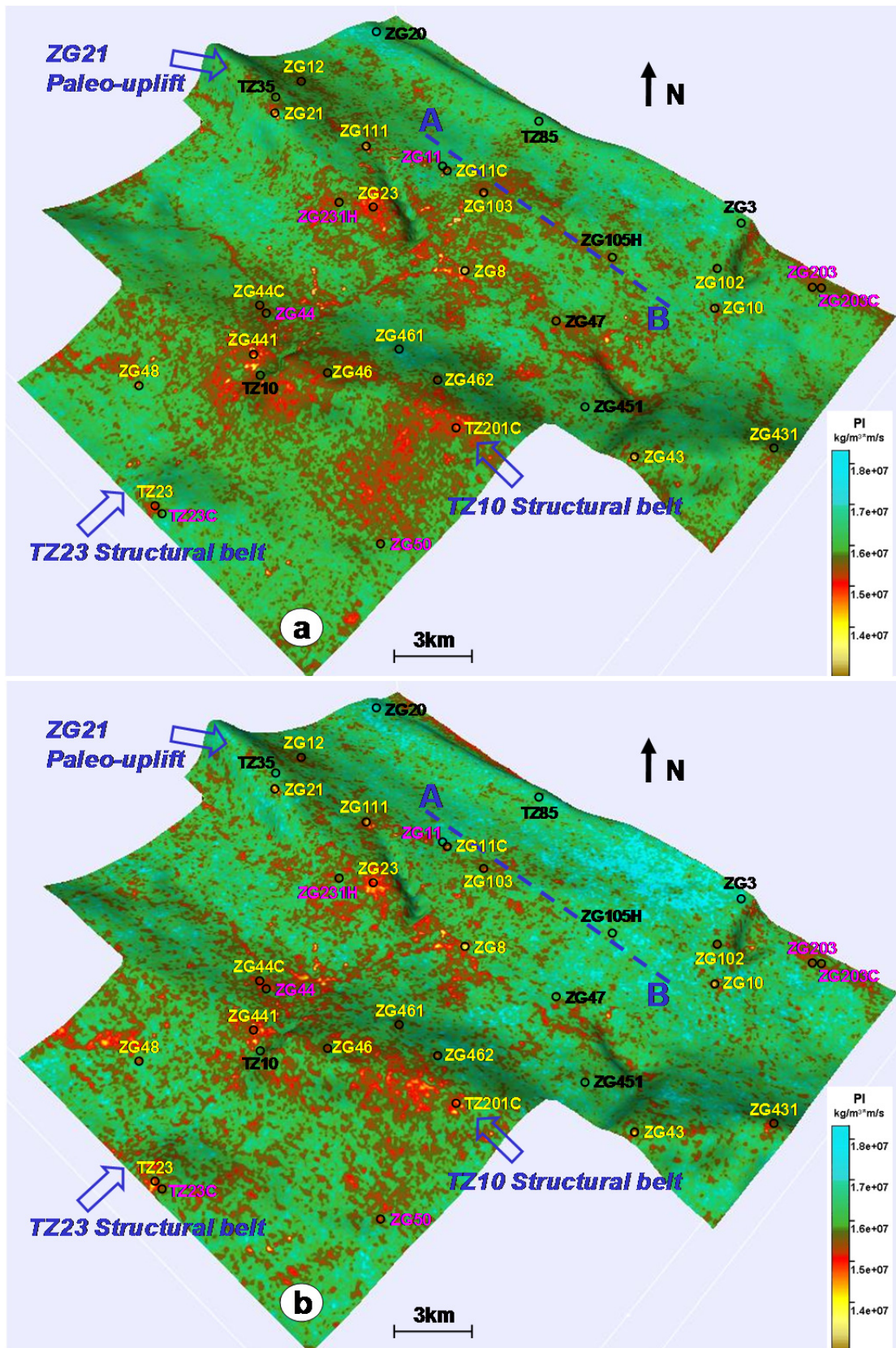


Figure 6. The comparison of the root mean square attribute of inverted impedance in the first part of Yingshan fm, Ordovician, ZG8 area, respectively inverted from conventional full-stack (a) and inverted P-wave (b) data. The oil&gas producing, water producing and dry wells are respectively stamped by yellow, pink and dark colors

5. Conclusions

Although routinely used for reservoir prediction, the conventional full-stack data are usually contaminated by the AVO effects and could be inappropriate for the reservoir description, especially for the deeply buried carbonate reservoir in the Tarim Basin. The inverted P-wave data via AVO inversion have a higher resolution, and are obviously more beneficial for reservoir prediction and well deployment. In essence, the P-wave data inversion is an important complement to current processing strategy.

Acknowledgments

We appreciate Tarim Oilfield Co. for providing field data. And we would also like to thank Fugro-Jason and Paradigm for their software support.

References

- Castagna, J. P., Swan, H. W., & Foster, D. J. (1998). Framework for AVO gradient and intercept interpretation. *Geophysics*, 63, 948-956. <http://dx.doi.org/10.1190/1.1444406>
- Chen, G., Pan, W., Sa, L., Han, J., & Guan, W. (2005). Application of prediction techniques in carbonate karst reservoir in tarim basin. *Applied Geophysics*, 2, 111-118
- Dembicki, E. A., & Machel, H. G. (1996). Recognition and delineation of paleokarst zones by the use of wireline logs in the bitumen-saturated Upper Devonian Grosmont Formation of northeastern Alberta, Canada. *AAPG bulletin*, 80, 695-712.
- Feng, X., Wang, Y., Wang, X., Wang, N., Gao, G., & Zhu, X. (2012). The application of high-resolution 3D seismic acquisition techniques for carbonate reservoir characterization in China. *The Leading Edge*, 31, 168-179. <http://dx.doi.org/10.1190/1.3686914>
- Gidlow, P. M., Smith, G. C., & Vail, P. J. (1992). *Hydrocarbon detection using fluid factor traces: A case study*. Proceedings of the Joint SEG/EAGE Summer Research Workshop on "How Useful is Amplitude-Versus-Offset (AVO) Analysis?" (pp. 78-89).
- Han, J., Sun, S. Z., Zhang, X., Zhang, Y., Chen, J., Pan, Y., ... Zhao, H. (2013). *Integrated Identification for Complex Reservoir Based on Pure P-Wave Data and Post-Stack Data*. Proceedings of the 2013 SEG Conference & Exhibition, Houston, USA. <http://dx.doi.org/10.1190/segam2013-1287.1>
- Janson, X., Zeng, H., Loucks, B., John, A., Jackson, Y. G., Wang, Q., ... Xia, Y. (2010). *An Ultra-Deep Paleokarst System In the Ordovician North-Central Tarim Basin China: Outcrop Analog And Synthetic Seismic Models*. Proceedings of the 2010 SEG Conference & Exhibition, Denver, USA. <http://dx.doi.org/10.1190/1.3513132>
- Jia, D., Lu, H., Cai, D., Wu, S., Shi, Y., & Chen, C. (1998). Structural features of northern Tarim Basin: Implications for regional tectonics and petroleum traps. *AAPG bulletin*, 82, 147-159.
- Kerans, C. (1988). Karst-controlled reservoir heterogeneity in Ellenburger Group carbonates of west Texas. *AAPG bulletin*, 72, 1160-1183.
- Loucks, R. G. (1999). Paleocave carbonate reservoirs: origins, burial-depth modifications, spatial complexity, and reservoir implications. *AAPG bulletin*, 83, 1795-1834.
- Ping, Y., Yonglei, L., Yunpeng, H., Huiqing, J., Dong, L., & Haiying, L. (2007). *Carbonate Reservoirs Prediction Strategy And Technologies In Tarim Basin of China*. Proceedings of the 2007 SEG Conference & Exhibition, San Antonio, USA. <http://dx.doi.org/10.1190/1.2793035>
- Rutherford, S. R., & Williams, R. H. (1989). Amplitude-versus-offset variations in gas sands. *Geophysics*, 54, 680-688. <http://dx.doi.org/10.1190/1.1442696>
- Sun, S. Z., Wang, H., Liu, Z., Li, Y., Zhou, X., & Wang, Z. (2012). The theory and application of DEM-Gassmann rock physics model for complex carbonate reservoirs. *The Leading Edge*, 31, 152-158. <http://dx.doi.org/10.1190/1.3686912>
- Sun, S. Z., Yang, H., Zhang, Y., Han, J., Wang, D., Sun, W., & Jiang, S. (2011b). The application of amplitude-preserved processing and migration for carbonate reservoir prediction in the Tarim Basin, China. *Petroleum Science*, 8, 406-414.
- Sun, S., Zhou, X., Li, Y., Wang, H., & Zhang, Y. (2011a). *Fluid Identification of Caved Carbonate Reservoir Based on Prestack Inversion*. Proceedings of the 2011 EAGE Conference & Exhibition, Vienna, Austria. <http://dx.doi.org/10.3997/2214-4609.20149591>

- Tinker, S., Ehrets, J., & Brondos, M. (1995). Multiple karst events related to stratigraphic cyclicity: San Andres Formation, Yates field, west Texas. *AAPG Memoir*, 63, 213 – 237.
- Wang, X., Feng, X., Luo, W., Gao, X., & Zhu, X. (2012). Key issues and strategies for processing complex carbonate reservoir data in China. *The Leading Edge*, 31, 180-188. <http://dx.doi.org/10.1190/1.3686916>
- Yang, H., Xue, F., Pan, W., Chen, L., Yang, P., Tong, Y., & Zhao, C. (2010). *Seismic Description of Karst Topography And Caves of Ordovician Carbonate Reservoirs Lungu Area Tarim Basin West China*. Proceedings of the 2010 SEG Conference & Exhibition, Denver, USA. <http://dx.doi.org/10.1190/1.3513072>
- Yang, P., Sun, S. Z., Liu, Y., Li, H., Dan, G., & Jia, H. (2012). Origin and architecture of fractured-cavernous carbonate reservoirs and their influences on seismic amplitudes. *The Leading Edge*, 31, 140-150. <http://dx.doi.org/10.1190/1.3686911>
- Zeng, H., Wang, G., Janson, X., Loucks, R., Xia, Y., Xu, L., & Yuan, B. (2011). Characterizing seismic bright spots in deeply buried, Ordovician paleokarst strata, Central Tabei uplift, Tarim Basin, Western China. *Geophysics*, 76, 127-137. <http://dx.doi.org/10.1190/1.3581199>
- Zhang, Y., Sun, S. Z., Yang, H., Wang, H., Han, J., Gao, H., ... Jing, B. (2011a). Pre-stack inversion for caved carbonate reservoir prediction: A case study from Tarim Basin, China. *Petroleum Science*, 8, 415-421.
- Zhang, Y., Sun, Z., & Fan, C. (2013). *An Iterative AVO Inversion Workflow for S-wave Improvement*. Proceedings of the 2013 EAGE Conference & Exhibition, London, UK. <http://dx.doi.org/10.3997/2214-4609.20130268>
- Zhang, Y., Sun, Z., Yang, H., Tang, Z., Wang, H., & Bai, H. (2011b). *The Advantages of Pre-stack Inversion in Heterogeneous Carbonate Reservoir Prediction-A Case Study from Tarim Basin, China*. Proceedings of the 2011 EAGE Conference & Exhibition, Vienna, Austria. <http://dx.doi.org/10.3997/2214-4609.20149735>

Copyrights

Copyright for this article is retained by the author(s), with first publication rights granted to the journal.

This is an open-access article distributed under the terms and conditions of the Creative Commons Attribution license (<http://creativecommons.org/licenses/by/3.0/>).